Journal of Magnetic Resonance 300 (2019) 76–83

Contents lists available at ScienceDirect

Journal of Magnetic Resonance

journal homepage: www.elsevier.com/locate/jmr

ASAP-HSQC-TOCSY for fast spin system identification and extraction of long-range couplings

Johanna Becker [1], Martin R.M. Koos, David Schulze-Sünninghausen [2], Burkhard Luy

Institut für Organische Chemie and Institut für Biologische Grenzflächen, Karlsruher Institut für Technologie (KIT), Fritz-Haber-Weg 6, 76131 Karlsruhe, Germany

ARTICLE INFO

Article history:
Received 17 October 2018
Revised 19 December 2018
Accepted 20 December 2018
Available online 18 January 2019

Keywords:
ASAP
HSQC-TOCSY
IPAP
Fast NMR experiments
Long-range ^{1}H-^{13}C coupling constants

ABSTRACT

Based on Ernst-angle-type excitation and Acceleration by Sharing Adjacent Polarization (ASAP), a fast HSQC–TOCSY experiment is introduced. In the approach, the DIPSI–2 isotropic mixing period of the ASAP–HSQC is simply shifted, which provides a TOCSY period without additional application of rf-energy. The ASAP-HSQC-TOCSY allows the acquisition of a conventional 2D in about 30 s. Alternatively, it allows the acquisition of highly carbon-resolved spectra (several Hz digital resolution) on the order of minutes. An ASAP-HSQC-TOCSY-IPAP variant, finally, allows the sign-sensitive extraction of heteronuclear long-range coupling constants from a pair of highly resolved spectra in less than an hour. Pulse sequences, several example spectra, and a discussion of results are given.

1. Introduction

In liquid state NMR the two-dimensional HSQC-TOCSY [1–4] is a well-known experiment for the identification of spin systems. It is widely used for the analysis of constituents of either a single pure compound [5–7] or complex mixtures of molecules [8–11]. When required, it can be extended to a 3D experiment with an additional proton dimension to allow, e.g., the assignment of amino acid spin systems in peptides or proteins [12,13]. In modified versions, it is also used for the sign-sensitive measurement of heteronuclear long-range coupling constants [14–21].

The experiment is based on an HSQC sequence followed by a TOCSY mixing period such that the exceptional resolution of the heteronucleus (usually ^{13}C) in the indirect dimension is combined with the propagation of magnetization via $^{n}J_{HH}$ couplings throughout the spin system. Due to the grid of correlations, it is easy to identify the different spin systems and properly assign individual signals especially in cases with significant spectral overlap. As such, it is e.g. commonly used for the characterization of monomeric units of oligosaccharides. One of the most successful ways of measuring long-range coupling constants, on the other hand, involves the combination of the conventional inphase-detected (IP) experiment with an antiphase-detected (AP) experiment, which allows the separation of α and β components of multiplets [17,18,22–25].

However, to make full use of the heteronuclear resolution of an HSQC-TOCSY, a relatively large number of increments has to be recorded for the indirect dimension, leading to relatively long experiment times. As such, the combination of an HSQC-TOCSY with rapid acquisition approaches is highly desirable. Here, we combine the HSQC-TOCSY with the ASAP approach, which is particularly fruitful, as the TOCSY period can be simultaneously used for spread of acquired coherences as well as for spread of reservoir polarization. Corresponding pulse sequences for ASAP-HSQC-TOCSY variants for inphase and antiphase detection are introduced as well as several proof of principle examples regarding fast and/or highly resolved spin system analyses in a two-component mixture, a tetra saccharide, as well as sign-sensitive coupling measurement on a disaccharide, respectively.

2. Theory

For small molecules at natural abundance in particular two types of approaches lead to rapid acquisition of heteronuclear correlation experiments without significant loss in sensitivity, the ASAP [26–29] and the ALSOFAST [27,29–31] approach. Both methods enable fast repetition due to Ernst-angle-type excitation and the ASAP approach in addition uses isotropic mixing in between scans for a faster build-up of polarization. As such, the ASAP-HMQC [26] and ASAP-HSQC [27] sequences both contain already all elements of an HMQC/HSQC-TOCSY sequence. Hence proceed-

[1] Current address: Currenta GmbH & Co. OHG, 51368 Leverkusen, Germany.
[2] Current address: Bruker BioSpin GmbH, 76287 Rheinstetten, Germany.
E-mail address: Burkhard.Luy@kit.edu (B. Luy)

https://doi.org/10.1016/j.jmr.2018.12.021
1090-7807/

ing from the improved symmetrized version of the ASAP-HSQC recently published [29], development of the ASAP-HSQC-TOCSY sequence shown in Fig. 1A was straightforward. As already known from the published ASAP sequences [26–29] the essential feature of the approach is the selective excitation of all ^{13}C-bound protons, while storing all unused magnetization from active and passive protons along z. In the classical ASAP experiments this reservoir of spin polarization is distributed over all protons via a homonuclear mixing period after acquisition and directly before the following scan. For the ASAP-HSQC-TOCSY the mixing period is shifted before the acquisition of the FID, assuring the magnetization transfer through the whole spin system via J_{HH} couplings. If the right multiple pulse sequence is chosen for the isotropic mixing period, both the transfer of coherences as well as the transfer of reservoir polarization can be achieved. While classical isotropic mixing sequences like MLEV-16 [32,33], MLEV-17 [34], FLOPSY [35], or MOCCA-XY16 [36–38] fail to produce corresponding isotropic mixing conditions for I_x and I_z simultaneously, DIPSI-2 is well-known for achieving remarkable bandwidths for isotropic mixing conditions along all axes [39,40]. As a consequence, both desired transfers can be achieved straightforwardly and spreading of magnetization for spin system detection as well as fast build-up of polarization will allow the acquisition of ASAP-HSQC-TOCSY experiments with no additional rf-energy applied.

For the ASAP-HSQC version chosen for the construction of the ASAP-HSQC-TOCSY experiment (Fig. 1), the echo/antiecho-encoding is achieved by a pair of gradients of equal sign and strength. Flanking the t_1 incrementation period, the two gradients

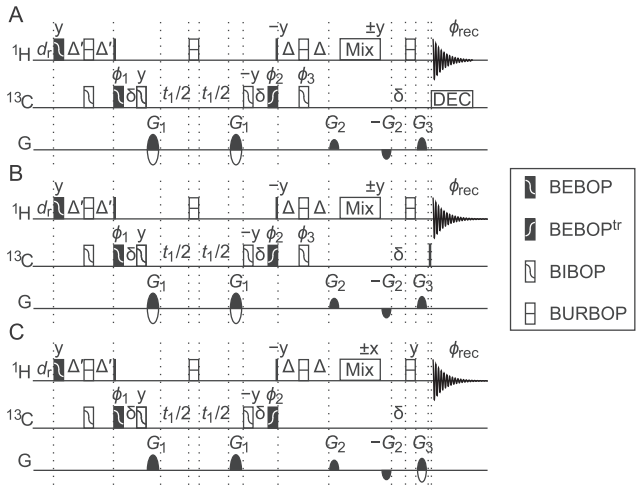

Fig. 1. ASAP-HSQC-TOCSY(-IPAP) pulse sequences: decoupled ASAP-HSQC-TOCSY (A), coupled inphase (IP, B), and anti-phase experiment (AP, C). Pulse phases are x unless indicated otherwise. Vertical lines represent 90° hard, black boxes represent 90° broadband pulses. Wide unfilled rectangles correspond to 180° broadband pulses. Where possible, pulse sequences were implemented using broadband excitation/time-reversed excitation/inversion pulses from the BEBOP/BIBOP family [42–46,48] and universal rotation pulses from the BURBOP family [50,52,53] as depicted in the legend and described in the experimental section. Usually, only a single scan is acquired but phase cycling can be implemented by ϕ_1 = 2(x), 2(−x); ϕ_2 = x, −x; ϕ_3 = x. IP and AP spectra are phase shifted by 90° therefore ϕ_{rec} = x, −x, −x, x (A) and ϕ_{rec} = y, −y, −y, y (B) are used. TPPI [56] was achieved by simultaneous inversion of phases ϕ_2 and ϕ_3. The delay $\Delta = 1/(4{\cdot}{}^1J_{CH})$ is typically set to an average coupling constant of 145 Hz. The delay $\Delta' = 1/(4{\cdot}210\,\text{Hz})$ is recommended as an initial guess for standard sample, but Δ' can be optimized individually for every sample as an Ernst angle equivalent [41]. The rectangle with the insert Mix indicates an isotropic mixing sequence which was implemented using the DIPSI-2 sequence [39], GARP [57] was used for decoupling. Gradients flanking the mixing sequence were set to G_2 = 33% of the maximum gradient strength (50.7 G/cm). For the decoupled and the IP sequence, echo/antiecho coherence order selection was achieved by gradient scheme G_1 = (40%, −40%), G_3 = (20.1%, 20.1%) while for the AP sequence, G_1 = (40%, 40%), G_3 = (20.1%, −20.1%) was used. Typical gradient durations are 1 ms for all gradient pulses with the delay δ balancing the length of gradient-free periods for symmetry.

produce a gradient echo for proton magnetization, thereby retaining transverse reservoir magnetization, as the following 90°$_y$ pulse on protons flips unused magnetization back along the z-axis. For Ernst-angle [41] type excitation the delay Δ' can be adjusted for the specific sample for optimal results as reported for the ALSOFAST-HMQC [30]. In most cases $\Delta' = 1/(4{\cdot}210\,\text{Hz})$ is close enough to the correct Ernst angle for maximum intensity. Finally, the DIPSI-2 mixing period is applied prior to echo/antiecho-decoding and acquisition. As reported for the already published ASAP-HSQC-sequences [27–29] best possible robustness of the sequences is achieved if broadband shaped pulses, e.g. optimal control-derived point-to-point [42–49] and universal rotation [50–55] pulses, are used (for details of pulses see experimental section).

The ASAP-HSQC-TOCSY sequence has been slightly modified for its use in the ASAP-HSQC-TOCSY-IPAP experiment. Fig. 1B and C show the two pulse sequences for the IP and AP subspectra. The IP-sequence equals the ASAP-HSQC-TOCSY without application of heteronuclear decoupling but with an additional carbon 90° pulse before acquisition, which converts eventually occurring dispersive antiphase contributions into non-detectable multi-quantum terms following the CLIP-approach [58,59]. The AP-sequence contains the same building blocks to assure that the two sequences are of identical length, which is crucial when the two spectra are combined to be able to extract $^nJ_{CH}$-coupling constants. In the AP-sequence the last 180° pulse of the back-transfer on the carbon channel is omitted, while the 180° pulse on protons is still applied, resulting in effective heteronuclear decoupling. The ^{1}H,^{13}C-antiphase magnetization on protons is conserved. The CLIP-pulse on the carbon channel is not applied, as it would destroy the antiphase magnetization.

3. Results and discussion

3.1. Proof of principle

As an initial proof of principle, the ASAP-HSQC-TOCSY pulse sequence was applied to a 500 mM menthol sample dissolved in $CDCl_3$. With a minimal delay between scans of only 1 ms and acquisition times of 152.4 ms and 4.2 ms, the 128-increment ASAP-HSQC-TOCSY could be recorded in only 30 s overall experiment time. The corresponding ^{1}H,^{13}C-correlation spectrum is displayed in Fig. 2A with the corresponding coupling pattern. Signals arising from directly coupled proton-carbon spin pairs, the classical HSQC correlations, are indicated with red circles. Clearly all desired correlations within the ring and the isopropyl group are visible.

In Fig. 2B then the application of the pulse sequence to a mixture of 300 mM menthol and norcamphor dissolved in $CDCl_3$ is shown. Again, the fast pulse sequence allowed the acquisition of an HSQC-TOCSY spectrum in 30 s. The two different spin systems could be easily identified. Blue lines in Fig. 2B indicate signals of norcamphor, whereas red dotted lines indicate correlations of menthol. It should be noted that the contour levels of the resulting HSQC-TOCSY spectra were chosen to also display correlations with low signal intensities. In doing so, also undesired F_1 ridges appear for intense methyl groups, which, however, do not impair the quality of the spectrum.

To show the efficiency of the ASAP method, the new experiment was compared to a state-of-the-art HSQC-SI-TOCSY. Fig. 3A shows the increased signal intensity of the ASAP-HSQC-TOCSY (black) over the conventional experiment (red) at short repetition times, while the two experiments are roughly equal with longer repetition times (B). Consequently, in the full spectrum shown in Fig. 3C, some correlations are only present in the ASAP-HSQC-TOCSY.

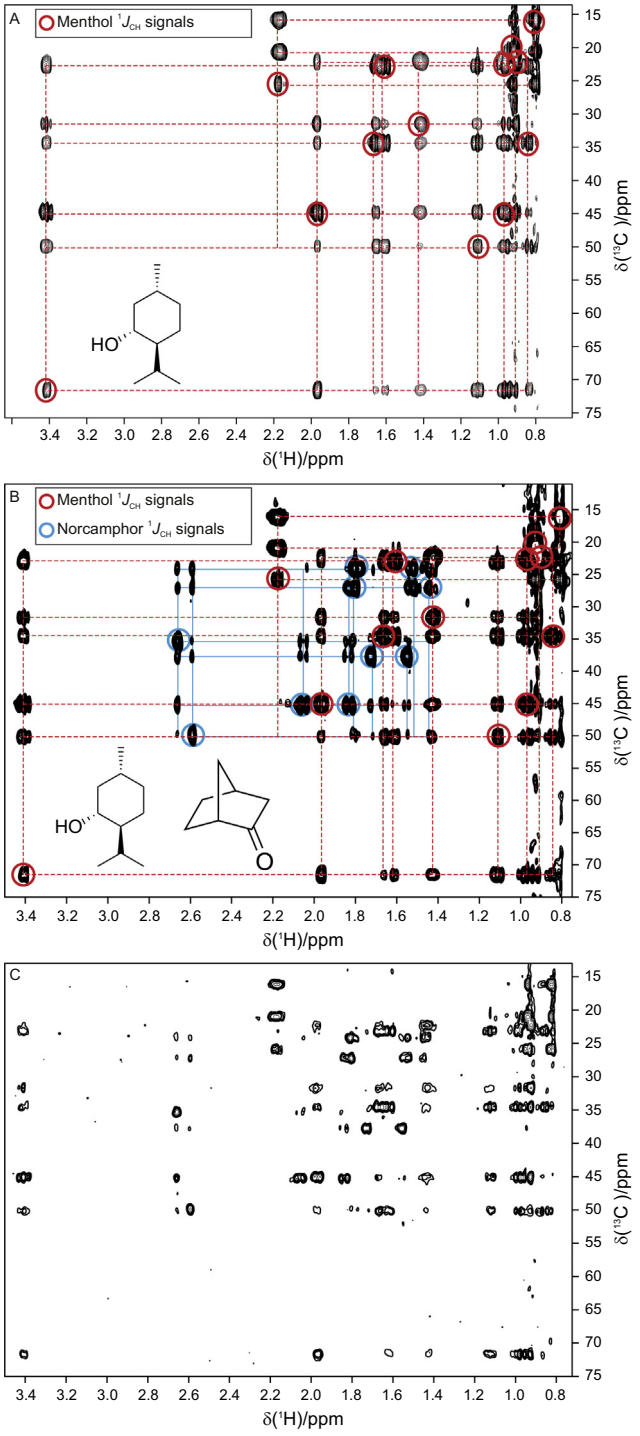

Fig. 2. HSQC-TOCSY spectra recorded with the ASAP-HSQC-TOCSY pulse sequence of Fig. 1A. (A) Spectrum of a 500 mM menthol sample in $CDCl_3$, (B) spectrum of a 300 mM mixture of menthol and norcamphor in $CDCl_3$, and (C) spectrum of the same mixture at 50 mM. For all spectra, 612 × 128 (t_2, t_1) real data points were recorded with 150 ms (t_2) and 4.2 ms (t_1) acquisition time, respectively. The experiments were acquired with 1 scan (A, B) or 2 scans (C) per t_1 increment and 16 dummy scans in 30 s (A, B) or 57 s (C) and processed using linear prediction as well as zero filling with twice the time domain points in both dimensions. In A and B, signals originating from $^1J_{CH}$ coupled spin pairs are marked by circles. To connect signals, blue lines show correlations of norcamphor, red dotted lines indicate correlations of menthol. (For interpretation of the references to colour in this figure legend, the reader is referred to the web version of this article.)

Further reduction of measurement time by the application of non-uniform sampling like in the ASAP-HSQC case failed in our hands. The large number of cross peaks along proton resonance

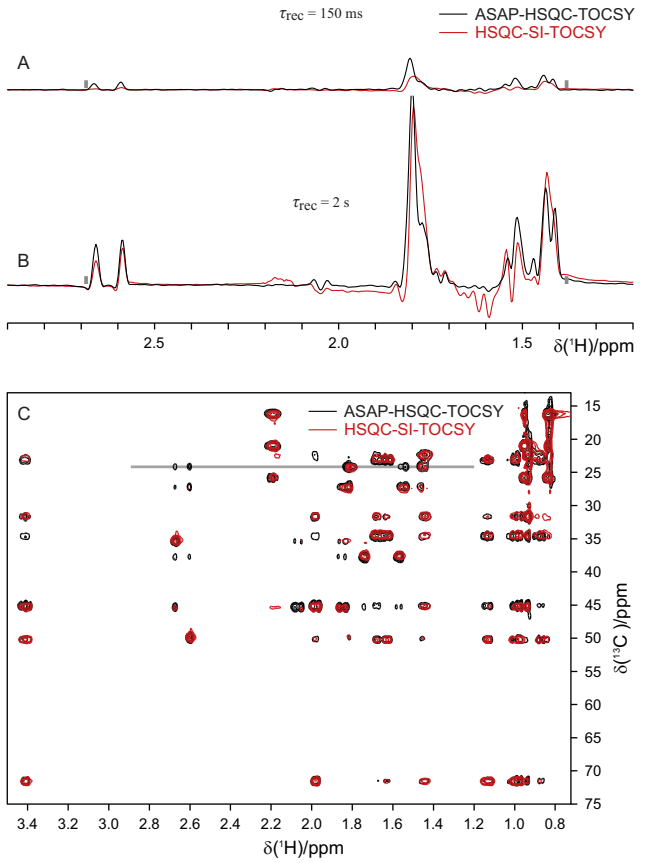

Fig. 3. Comparison of intensity and saturation of ASAP-HSQC-TOCSY (black) and conventional HSQC-SI-TOCSY (red), acquired on a 300 mM menthol/norcamphor mixture in $CDCl_3$. (A) F_2 traces of experiments with τ_{rec} = 150 ms (τ_{rec} = acquisition time + delay d_r) extracted at $\delta(^{13}C)$ = 24.4 ppm. (B) F_2 traces of experiments with τ_{rec} = 2 s at $\delta(^{13}C)$ = 24.4 ppm. Grey bars are included as a guide to the eye to compare the intensities. (C) Full spectra with τ_{rec} = 150 ms, 612 × 128 (t_2, t_1) points were acquired with 1 scan per increment in 30 s, the grey line marks the origin of the traces in A. Spectra with τ_{rec} = 2 s (not shown) were acquired at the same resolution in 5 min.

frequencies in this experiment requires a very high sampling density close to 100%.

3.2. Spin system identification at high resolution

As has been reported previously [27–29], the ASAP approach can also be used for acquiring spectra with very high resolution in reasonably short experiment times. An example is shown in Fig. 4, where the tetra saccharide stachyose has been subject of spin system identification using the ASAP-HSQC-TOCSY. As with many oligosaccharides, considerable overlap with chemical shift differences in the low ppb range in the proton as well as carbon dimension are observed. Accordingly, spectra have to be acquired with high resolution especially in the indirect dimension, where sharp ^{13}C-singlets will have the highest probability to differentiate individual resonances.

An ASAP-HSQC-TOCSY spectrum has been recorded with 512 × 1024 (t_2, t_1) real data points and processed using linear prediction and zero filling to 2048 × 4192 real points, leading to a digital resolution in the indirect dimension of 3.7 Hz – in an overall measurement time of less than four minutes. Especially the insert in Fig. 4, with the most heavily crowded region, shows that all resonances can be distinguished, even if the closest pair of resonances with only 3.6 Hz difference partially overlaps.

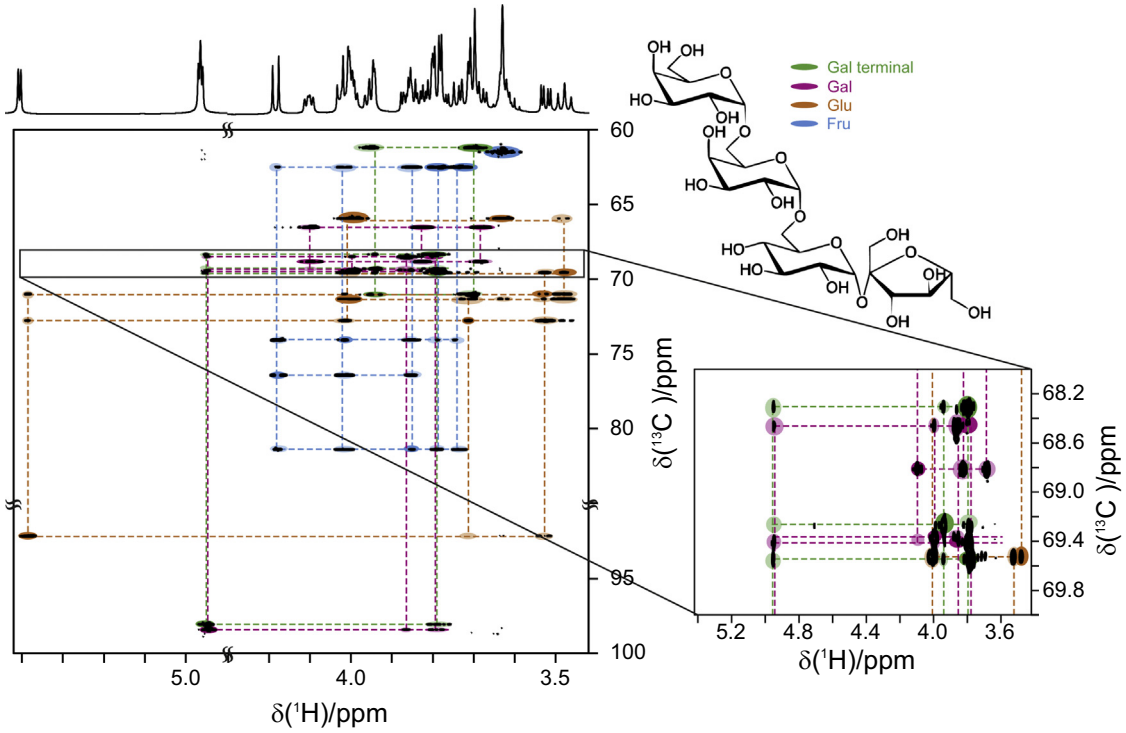

Fig. 4. ASAP-HSQC-TOCSY spectrum of a 250 mM stachyose sample in D_2O. 512 × 1024 (t_2, t_1) data points were recorded corresponding to acquisition times of 106.7 ms and 67.9 ms, respectively. The experiment was acquired using 1 scan per t_1 increment and 16 dummy scans in altogether 3 min and 25 s. Linear prediction and zero filling with twice the time domain points in both dimensions was applied to process the spectrum, resulting in a digital resolution in the indirect dimension of 3.7 Hz. As a consequence, the smallest frequency difference of 3.6 Hz is resolved, although cross peaks at approximately 69.4 ppm partially overlap. The expanded area shows the most critical area. The patterns of correlation for the four sugars are highlighted with the colour code given next to the structure of stachyose.

3.3. Determination of long-range couplings

Sign-sensitive measurement using the IPAP principle relies on spin state selectivity, requiring the acquisition of two different data sets and combining them to separate α/β multiplet components in two subspectra [21,25,60,61]. In contrast to a fully coupled spectrum, the two combined subspectra contain only one half of the multiplet, thereby reducing the overall signal overlap. In combination with a TOCSY mixing period spreading of magnetization allows to obtain $^nJ_{CH}$ coupling constants in a sign-sensitive way, as resulting α or β components can be referenced to the one-bond signal with positive $^1J_{CH}$ value. As such, the HSQC-TOCSY-IPAP experiment is capable to measure long-range heteronuclear coupling constants, which is of particular interest to the structure determination of small-to-medium-sized organic molecules. In addition, also long-range residual dipolar couplings in principle may be determined using partially aligned samples. Needless to say that the coupling measurement is limited to protonated X-nuclei; all other couplings have to be measured using a different experimental approach such as HMBC-type experiments [25,62–67].

With the ASAP-HSQC-TOCSY-IPAP sequences shown in Fig. 1B and C a fast approach applicable to the extraction of long-range couplings is accessible. Using the simple test molecule glucose in D_2O, their power to acquire spectra with high resolution in the indirect dimension is demonstrated. As for reliable coupling measurements signals must be baseline-separated in the indirect dimension, a high digital resolution is needed.

Since the IP-sequence consists of two INEPT-type transfer elements, while the AP-sequence possesses only one such heteronuclear transfer step, the IP is more error prone to mismatched delays than the AP. However, to avoid errors in the coupling extraction, the relative intensities of IP and AP subspectra can be corrected by using cross peaks originating from one-bond correlations. The example considered herein shows a very narrow distribution of $^1J_{CH}$-coupling constants and with one exception, IP and AP spectra were of same intensities and could simply be added/subtracted, resulting in two subspectra from which the $^nJ_{CH}$-coupling constants could be extracted (Fig. 5C and example cross peaks with opposite sign in Fig. S2 of the supporting information). The only exception was the C5α position, where the difference of the relative intensity was compensated by scaling to two subspectra to equal intensity of the ^1J peaks. Corresponding coupling constants are summarized in Table 1, where they are also compared to a conventional HSQC-TOCSY-IPAP [25,61] that was acquired in over four hours. Extracted couplings generally differ only slightly within the narrow error margins derived from experiment.

Next to the considerable results and the extraordinary reduction in measurement time also two potentially occurring artefacts should be pointed out:

It is well known, that coupling extraction could be hampered by homonuclear coupling evolution, resulting in dispersive antiphase contributions. While such distortions can be obvious in the original spectra, their effect on the calculated sum and difference subspectra can be less obvious but still affecting the coupling determination. In the spectra acquired with the conventional experiment [25] such phase distortions are reduced due to the z-filter elements for zero quantum suppression used around the TOCSY mixing period [68], which is not possible in the ASAP experiment. In practice, however, we could not see that the phase-distortions of multiplet components led to any problems in coupling extraction.

In addition, we encountered two cases (one in the fast ASAP-HSQC-TOCSY-IPAP, one in the conventional HSQC-TOCSY-IPAP), where linear prediction caused extrapolation artefacts severely

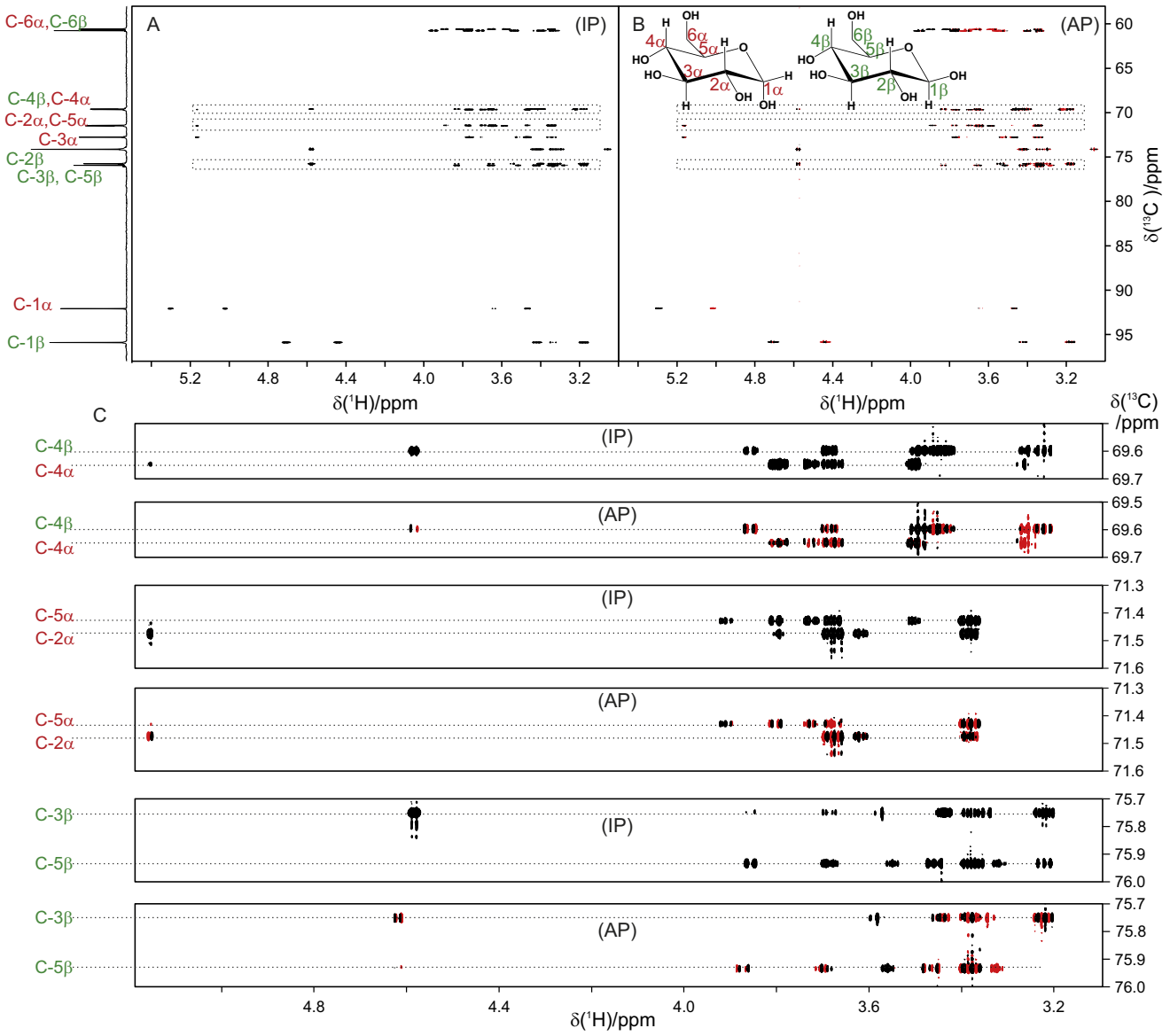

Fig. 5. ω_2-coupled ^{1}H,^{13}C-ASAP-HSQC-TOCSY in-phase (IP, A) and ^{1}H,^{13}C-ASAP-HSQC-TOCSY anti-phase (AP, B) spectrum of a 350 mM glucose sample in D_2O recorded with the ASAP-HSQC-TOCSY-IPAP sequences shown in Fig. 1B and C. For coupling extraction, acquisition and procession parameters were kept equal. The experiments were performed with a resolution of 2048 × 4096 (t_2, t_1) real data points corresponding to acquisition times of 569.3 ms and 226.3 ms for the two dimensions. 1 scan per t_1 increment and 4 dummy scans were acquired in altogether 50 min and 33 s. The spectra were processed using linear prediction and zero filling with twice the time domain points in both dimensions. Distinction of the signals of α- and β-glucose is even possible in the expanded areas of both the IP and AP spectra with differences in carbon chemical shifts as small as 7.3 Hz (C).

affecting the shape of small signals. Coupling determination was therefore performed on spectra processed without linear prediction for these signals.

4. Experimental

All NMR spectra were recorded on a 600 MHz Bruker Avance III spectrometer equipped with a ^{1}H,^{13}C,^{15}N-TCI cryogenically cooled probe head optimized for ^{1}H-detection at a temperature of 300 K. Spectra were acquired on various model samples: a 500 mM menthol/$CDCl_3$ sample, a mixture of 300 mM menthol and 300 mM norcamphor in $CDCl_3$, a mixture of 50 mM menthol and 50 mM norcamphor in $CDCl_3$, a 250 mM stachyose/D_2O sample, and a 350 mM glucose/D_2O sample. All solutes were used at natural-abundance isotope level.

Filled rectangles on the ^{1}H and ^{13}C channel in Fig. 1 mark a BEBOP(10 kHz, 20 kHz, 550 μs, ±20%, 1100) [54] (^{1}H) or a BEBOP (37.5 kHz, 10 kHz, 550 μs, ±5%, 1100) (^{13}C) pulse using the nomenclature introduced in Ref. [52]; for simultaneous refocusing on protons and broadband inversion on carbon coupling-compensated 600 μs BUBI pulse sandwiches for best overall performance were applied [51,54,55]. The proton pulse of the sandwich is also used as a BURBOP-180x (10 kHz, 20 kHz, 600 μs, ±20%, 1200) [54] while the ^{13}C pulse is also used as a BIBOP (37.5 kHz, 10 kHz, 600 μs, ±5%, 1200) pulse [54]. All proton shaped pulses are applied with an rf-amplitude of 20 kHz, corresponding to a 90° hard pulse of 12.5 μs, carbon shaped pulses with an rf-amplitude of 10 kHz, corresponding to a 90° hard pulse of 25 μs. All magnetic field gradient pulses were z-gradients of 1 ms length, except for the spectra with high-concentration in Fig. 2A and B, where slightly better results were achieved with 1.5 ms.

Table 1
Measured long-range couplings of α/β-glucose obtained from a conventional HSQC-TOCSY-IPAP and the ASAP-HSQC-TOCSY-IPAP spectra displayed in Fig. 5.[1]

Correlation	$^{n}J_{CH}$	$^{n}J_{CH}$ (conv.) [Hz]	$^{n}J_{CH}$ (ASAP) [Hz]
C1α-H2α	$^{2}J_{CH}$	−0.82 ± 0.10	−0.82 ± 0.10
C1α-H3α	$^{3}J_{CH}$	0.86 ± 0.10	0.85 ± 0.10
C1β-H2 β	$^{2}J_{CH}$	−6.23 ± 0.10	−6.25 ± 0.10
C1β-H3β	$^{3}J_{CH}$	1.14 ± 0.10	1.18 ± 0.10
C2α-H1α	$^{2}J_{CH}$	−0.94 ± 0.10	−1.09 ± 0.10
C2α-H3α	$^{2}J_{CH}$	−4.30 ± 0.10	−4.26 ± 0.10
C2α-H4α	$^{3}J_{CH}$	0.90 ± 0.20	—
C2β-H1β	$^{2}J_{CH}$	0.81 ± 0.10	0.85 ± 0.10
C2β-H3β	$^{2}J_{CH}$	−4.75 ± 0.20	−4.58 ± 0.10
C2β-H4β	$^{3}J_{CH}$	0.68 ± 0.10	0.70 ± 0.10
C3α-H1α	$^{3}J_{CH}$	5.37 ± 0.20	5.38 ± 0.10
C3α-H2α	$^{2}J_{CH}$	−4.35 ± 0.20	−4.25 ± 0.10
C3α-H4α	$^{2}J_{CH}$	−4.39 ± 0.30	−4.40 ± 0.10
C3β-H1β	$^{3}J_{CH}$	0.96 ± 0.20	1.01 ± 0.10
C3β-H2β	$^{2}J_{CH}$	−4.73 ± 0.30	−4.61 ± 0.10
C3β-H4β	$^{2}J_{CH}$	−5.38 ± 0.30	−5.38 ± 0.20
C3β-H5β	$^{3}J_{CH}$	2.26 ± 0.20	2.37 ± 0.10
C4α-H1α	$^{3}J_{CH}$	−0.62 ± 0.20	−0.58 ± 0.10
C4α-H2α	$^{2}J_{CH}$	0.76 ± 0.20	0.82 ± 0.10
C4α-H3α	$^{2}J_{CH}$	−4.38 ± 0.10	−4.29 ± 0.20
C4α-H6′α	$^{2}J_{CH}$	0.87 ± 0.20	0.89 ± 0.30
C4β-H1β	$^{4}J_{CH}$	0.28 ± 0.10	0.44 ± 0.10
C4β-H2β	$^{3}J_{CH}$	0.79 ± 0.20	1.07 ± 0.10
C4β-H5β	$^{2}J_{CH}$	−3.84 ± 0.20	−3.89 ± 0.10
C4β-H6β	$^{3}J_{CH}$	2.50 ± 0.10	2.64 ± 0.10
C4β-H6′β	$^{3}J_{CH}$	1.30 ± 0.10	1.30 ± 0.10
C5α-H1α	$^{5}J_{CH}$	6.54 ± 0.30	6.71 ± 0.10
C5α-H3α	$^{3}J_{CH}$	0.94 ± 0.20	0.86 ± 0.10
C5α-H4α	$^{2}J_{CH}$	−3.90 ± 0.20	−3.83 ± 0.10
C5α-H6α	$^{2}J_{CH}$	−1.62 ± 0.10	−1.53 ± 0.10
C5α-H6′α	$^{2}J_{CH}$	−1.85 ± 0.10	−1.89 ± 0.10
C5β-H1β	$^{5}J_{CH}$	1.15 ± 0.10	1.30 ± 0.10
C5β-H3β	$^{3}J_{CH}$	0.92 ± 0.10	1.10 ± 0.10
C5β-H4β	$^{2}J_{CH}$	−4.79 ± 0.10	−4.82 ± 0.10
C5β-H6β	$^{2}J_{CH}$	−1.18 ± 0.10	−1.17 ± 0.10
C5β-H6′β	$^{2}J_{CH}$	−2.27 ± 0.10	−2.30 ± 0.10
C6α-H1α	$^{6}J_{CH}$	*0.14 ± 0.30	−0.09 ± 0.10
C6α-H4α	$^{3}J_{CH}$	3.59 ± 0.10	3.81 ± 0.20
C6α-H5α	$^{2}J_{CH}$	−1.72 ± 0.40	−1.59 ± 0.10
C6β-H2β	$^{5}J_{CH}$	0.31 ± 0.10	*0.31 ± 0,20
C6β-H4β	$^{3}J_{CH}$	3.36 ± 0.10	3.48 ± 0.10
C6β-H5β	$^{2}J_{CH}$	−1.95 ± 0.20	−1.97 ± 0.10

[1] Values are compared coupling constants extracted with reference HSQC-TOCSY-IPAP sequences of Ref. [25]. The procedure of coupling determination is explained in the supporting information. Values marked with an asterisk were extracted from spectra processed without linear prediction.

For Hartmann-Hahn mixing a DIPSI-2 sequence [39] with an rf-amplitude of 5 kHz was used. The mixing time was 34.53 ms. ASAP-experiments were acquired using 1 scan per t_1 increment and only 1 ms additional relaxation delay in between subsequent scans. The delay of the INEPT transfer element Δ′ was optimized according to the Ernst-angle [41] approach, as reported originally for the ALSOFAST-HMQC [30]. For menthol the delay was set according to $\Delta' = 1/(4J)$, with the optimized coupling constant of $J = 208$ Hz. The optimal value for the mixture of menthol and norcamphor turned out to be $J = 210$ Hz and $J = 200$ Hz for the two different sugar samples. The conventional HSQC-TOCSY-IP/AP experiments as described in Ref. [25] were recorded with 2048 × 4096 (t_2, t_1) real data points, and 0.57 s/0.23 s acquisition time in 4 h 15 min 8 s. Two scans were acquired per t_1 increment with 1 s additional relaxation delay in between subsequent scans. The INEPT transfer delay was $\Delta = 1/(4 \cdot 145\ \text{Hz})$, the TOCSY mixing time was 57.5 ms. For ^{13}C, in the conventional HSQC-TOCSY-IPAP the same shaped pulses as in the ASAP version were used, the two Thrippleton-Keeler-type z-filter elements were set to 30 ms and 50 ms length [68].

Heteronuclear decoupling was achieved using GARP [57]. For the measurement of long-range heteronuclear couplings, decoupling is omitted during acquisition. For each fast experiment complex data acquisition in the indirect dimension was obtained using the echo/antiecho method. For the state-of-the-art HSQC-SI-TOCSY for the comparison in Fig. 3, the Bruker pulse sequence HSQCDIETGPSISP was utilized with recommended parameters. Conventional HSQC-TOCSY spectra recorded to validate the coupling determination were acquired with the States/TPPI [69] protocol.

Processing was performed using Bruker TopSpin 3.5. Complex linear forward prediction of time domain data and zero filling to twice the number of data points in both dimensions was utilized whenever mentioned in the figure caption. The FIDs were multiplied with a π/2-shifted sine-squared window function and Fourier transformed. An automated baseline correction in both dimensions was performed and spectra were phased to absorption.

Like in previous works, the high duty cycle of the experiment has to be considered, which in principle can cause hardware damage. All of the aspects discussed in Ref. [29] are valid for the ASAP-HSQC-TOCSY with heteronuclear decoupling as well. While we encountered no problems with a cryogenically cooled probe, the effect on room temperature probes is difficult to ascertain and higher d_r is recommended. At, e.g., 100 ms ASAP still provides significant signal enhancement. Switching to low-power decoupling methods like adiabatic decoupling is also possible [70–72]. The IP/AP sequences without heteronuclear decoupling have lower rf power and pose a smaller risk.

5. Conclusion

We have presented the ASAP-HSQC-TOCSY experiment which allows the fast acquisition of complete ^{1}H,^{13}C-HSQC-TOCSY spectra of small molecules at natural abundance in as little as 30 s. It is elegantly based on the ASAP approach by shifting the ASAP mixing period in front of the acquisition, where it serves simultaneously for TOCSY transfer and polarization equilibration.

With the experiment, we provide a very fast approach suited for mixture analyses – more specifically the distinction and identification of spin systems. We gave one example of a mixture containing menthol and norcamphor. For the investigation of a tetra saccharide, high resolution in the indirect dimension was needed. Due to the fast repetition rate inherent to ASAP-type experiments, a digital ^{13}C resolution of 3.68 Hz could be achieved in only 3 min and 25 s. With this resolution it was possible to fully map the correlation pattern of the four sugars even though there were very similar chemical shifts with partially overlapping signals. With this high resolution it was even possible to identify all resonances of the two galactose monomers that only differ in their glycosidic linkage neighbors.

The ASAP-HSQC-TOCSY experiment has further been modified to give the ASAP-HSQC-TOCSY-IPAP experiments that are suitable for fast measurement of long-range proton-carbon couplings in small molecules providing the sign with reference to the large one-bond proton-carbon coupling and the size of the coupling constants. The experiment time for the acquisition of each data set for a 350 mM glucose sample in D_2O is 50 min and 33 s. Compared to the ASAP-HSQC-TOCSY experiment the increased overall measurement time is due to the long acquisition time in the direct dimension, which is needed for the antiphase magnetization to develop into detectable magnetization components. However, compared to the experiment time of the conventional approach of 4 h 15 min and 8 s the duration is still drastically reduced.

In summary, the presented ASAP-type HSQC-TOCSY sequences allow a significant speedup of the well-known correlation experiment. If the proper mixing sequence is used, the ASAP-HSQC-TOCSY experiments can be used for spin system

identification, mixture analysis, and even the sign-sensitive measurement of coupling constants as its conventional counterpart.

Competing interests

The authors have no competing interest to declare.

Acknowledgments

J.B. thanks the Fonds der Chemischen Industrie for a PhD fellowship. All authors thank the Deutsche Forschungsgemeinschaft (DFG) (instrumentation facility Pro^{2}NMR, LU 835/13-1, FOR 2290, and SFB 1176 projects A1 and Q2), the HGF programme BioInterfaces in Technology and Medicine for financial support.

Appendix A. Supplementary material

Supplementary data associated with this article can be found, in the online version, at https://doi.org/10.1016/j.jmr.2018.12.021.

References

[1] L. Lerner, A. Bax, Sensitivity-enhanced two-dimensional heteronuclear relayed coherence transfer NMR spectroscopy, J. Magn. Reson. 69 (1986) (1969) 375–380, https://doi.org/10.1016/0022-2364(86)90091-0, https://www.sciencedirect.com/science/article/pii/0022236486900910.

[2] T.J. Norwood, J. Boyd, I.D. Campbell, Improved resolution in ^{1}H-detected ^{1}H–^{15}N correlation experiments, FEBS Lett. 255 (1989) 369–371, https://doi.org/10.1016/0014-5793(89)81124-X, https://febs.onlinelibrary.wiley.com/doi/abs/10.1016/0014-5793(89)81124-X.

[3] G. Otting, H. Senn, G. Wagner, K. Wüthrich, Editing of 2D ^{1}H NMR spectra using X half-filters. Combined use with residue-selective ^{15}N labeling of proteins, J. Magn. Reson. 70 (1986) (1969) 500–505, https://doi.org/10.1016/0022-2364(86)90144-7, https://www.sciencedirect.com/science/article/pii/0022236486901447.

[4] G. Otting, K. Wüthrich, Efficient purging scheme for proton-detected heteronuclear two-dimensional NMR, J. Magn. Reson. 76 (1988) (1969) 569–574, https://doi.org/10.1016/0022-2364(88)90361-7, https://www.sciencedirect.com/science/article/pii/0022236488903617.

[5] J.Ø. Duus, C.H. Gotfredsen, K. Bock, Carbohydrate structural determination by NMR spectroscopy: modern methods and limitations, Chem. Rev. 100 (2000) 4589–4614, https://doi.org/10.1021/cr990302n, https://pubs.acs.org/doi/abs/10.1021/cr990302n.

[6] K.E. Kövér, L. Szilágyi, G. Batta, D. Uhrín, J. Jiménez-Barbero, 907 – biomolecular recognition by oligosaccharides and glycopeptides: the NMR point of view, in: H.-W. Liu, L. Mander (Eds.), Comprehensive Natural Products II, Elsevier, Oxford, 2010, pp. 197–246, https://doi.org/10.1016/B978-008045382-8.00193-3.

[7] T. Gyöngyösi, I. Timári, J. Haller, M.R.M. Koos, B. Luy, K.E. Kövér, Boosting the NMR assignment of carbohydrates with clean in-phase correlation experiments, ChemPlusChem 83 (2018) 53–60, https://doi.org/10.1002/cplu.201700452, https://onlinelibrary.wiley.com/doi/abs/10.1002/cplu.201700452.

[8] W. Willker, D. Leibfritz, Assignment of mono- and polyunsaturated fatty acids in lipids of tissues and body fluids, Magn. Reson. Chem. 36 (1998) S79–S84, https://doi.org/10.1002/(SICI)1097-458X(199806)36:13<S79::AID-OMR294>3.0.CO;2-Z, https://onlinelibrary.wiley.com/doi/abs/10.1002/(SICI)1097-458X(199806)36:13<S79::AID-OMR294>3.0.CO;2-Z.

[9] K. Bingol, L. Bruschweiler-Li, D.-W. Li, R. Brüschweiler, Customized metabolomics database for the analysis of NMR ^{1}H–^{1}H TOCSY and ^{13}C–^{1}H HSQC-TOCSY spectra of complex mixtures, Anal. Chem. 86 (2014) 5494–5501, https://doi.org/10.1021/ac500979g, https://pubs.acs.org/doi/10.1021/ac500979g.

[10] W. Kew, N.G.A. Bell, I. Goodall, D. Uhrín, Advanced solvent signal suppression for the acquisition of 1D and 2D NMR spectra of Scotch Whisky, Magn. Reson. Chem. 55 (2017) 785–796, https://doi.org/10.1002/mrc.4621, https://onlinelibrary.wiley.com/doi/abs/10.1002/mrc.4621.

[11] N. Brodaczewska, Z. Košťálová, D. Uhrín, (3, 2)D ^{1}H, ^{13}C BIRD^{r,} X-HSQC-TOCSY for NMR structure elucidation of mixtures: application to complex carbohydrates, J. Biomol. NMR 70 (2018) 115–122, https://doi.org/10.1007/s10858-018-0163-8, https://link.springer.com/article/10.1007/s10858-018-0163-8.

[12] A.S. Edison, W.M. Westler, J.L. Markley, Elucidation of amino acid spin systems in proteins and determination of heteronuclear coupling constants by carbon-proton-proton three-dimensional NMR, J. Magn. Reson. 92 (1991) (1969) 434–438, https://doi.org/10.1016/0022-2364(91)90285-2, URL: https://www.sciencedirect.com/science/article/pii/0022236491902852.

[13] M. Sattler, H. Schwalbe, C. Griesinger, Stereospecific assignment of leucine methyl groups with carbon-13 in natural abundance or with random ^{13}C labeling, J. Am. Chem. Soc. 114 (1992) 1126–1127, https://doi.org/10.1021/ja00029a072, https://pubs.acs.org/doi/abs/10.1021/ja00029a072.

[14] M. Kurz, P. Schmieder, H. Kessler, HETLOC, an efficient method for determining heteronuclear long-range couplings with Heteronuclei in natural abundance, Angew. Chem. Int. Ed. Engl. 30 (1991) 1329–1331, https://doi.org/10.1002/anie.199113291, https://onlinelibrary.wiley.com/doi/abs/10.1002/anie.199113291.

[15] U. Wollborn, D. Leibfritz, Measurements of heteronuclear long-range coupling constants from inverse homonuclear 2D NMR spectra, J. Magn. Reson. 98 (1992) (1969) 142–146, https://doi.org/10.1016/0022-2364(92)90117-P, https://www.sciencedirect.com/science/article/pii/002223649290117P.

[16] G. Xu, J.S. Evans, Determination of long-range J_{XH} couplings using "Excitation-Sculpting" gradient-enhanced heteronuclear correlation experiments, J. Magn. Reson., Ser A 123 (1996) 105–110, https://doi.org/10.1006/jmra.1996.0219, https://www.sciencedirect.com/science/article/pii/S1064185896902193.

[17] A. Meissner, J.Ø. Duus, O.W. Sørensen, Integration of spin-state-selective excitation into 2D NMR correlation experiments with heteronuclear ZQ/2Q π rotations for $^1J_{XH}$, J. Biomol. NMR 10 (1997) 89–94, https://doi.org/10.1023/a:1018331001961.

[18] M.D. Sørensen, A. Meissner, O.W. Sørensen, Spin-state-selective coherence transfer via intermediate states of two-spin coherence in IS spin systems: application to E.COSY-type measurement of J coupling constants, J. Biomol. NMR 10 (1997) 181–186, https://doi.org/10.1023/a:1018323913680, https://link.springer.com/article/10.1023/A:1018323913680.

[19] D. Uhrín, G. Batta, V.J. Hruby, P.N. Barlow, K.E. Kövér, Sensitivity- and gradient-enhanced hetero (ω_1) half-filtered TOCSY experiment for measuring long-range heteronuclear coupling constants, J. Magn. Reson. 130 (1998) 155–161, https://doi.org/10.1006/jmre.1997.1308, URL.

[20] P. Nolis, T. Parella, Spin-edited 2D HSQC–TOCSY experiments for the measurement of homonuclear and heteronuclear coupling constants: application to carbohydrates and peptides, J. Magn. Reson. 176 (2005) 15–26, https://doi.org/10.1016/j.jmr.2005.05.007, https://www.sciencedirect.com/science/article/pii/S109078070500162X.

[21] P. Nolis, J.F. Espinosa, T. Parella, Optimum spin-state selection for all multiplicities in the acquisition dimension of the HSQC experiment, J. Magn. Reson. 180 (2006) 39–50, https://doi.org/10.1016/j.jmr.2006.01.003, https://www.sciencedirect.com/science/article/pii/S1090780706000085.

[22] M. Ottiger, F. Delaglio, A. Bax, Measurement of J and dipolar couplings from simplified two-dimensional NMR spectra, J. Magn. Reson. 131 (1998) 373–378, https://doi.org/10.1006/jmre.1998.1361, https://www.sciencedirect.com/science/article/pii/S1090780798913611.

[23] T. Carlomagno, W. Peti, C. Griesinger, A new method for the simultaneous measurement of magnitude and sign of $^1D_{CH}$ and $^1D_{HH}$ dipolar couplings in methylene groups, J. Biomol. NMR 17 (2000) 99–109, https://doi.org/10.1023/a:1008346902500, https://link.springer.com/article/10.1023/A:1008346902500.

[24] B. Luy, Spin state selectivity and heteronuclear Hartmann-Hahn transfer, J. Magn. Reson. 168 (2004) 210–216, https://doi.org/10.1016/j.jmr.2004.03.005, https://www.sciencedirect.com/science/article/pii/S1090780704000618.

[25] K. Kobzar, B. Luy, Analyses, extensions and comparison of three experimental schemes for measuring ($^nJ_{CH}$+D_{CH})-couplings at natural abundance, J. Magn. Reson. 186 (2007) 131–141, https://doi.org/10.1016/j.jmr.2007.02.005, https://www.sciencedirect.com/science/article/pii/S1090780707000468.

[26] E. Kupče, R. Freeman, Fast multidimensional NMR by polarization sharing, Magn. Reson. Chem. 45 (2007) 2–4, https://doi.org/10.1002/mrc.1931, https://onlinelibrary.wiley.com/doi/abs/10.1002/mrc.1931.

[27] D. Schulze-Sünninghausen, J. Becker, B. Luy, Rapid heteronuclear single quantum correlation NMR spectra at natural abundance, J. Am. Chem. Soc. 136 (2014) 1242–1245, https://doi.org/10.1021/ja411588d, https://pubs.acs.org/doi/10.1021/ja411588d.

[28] J. Becker, B. Luy, CLIP–ASAP-HSQC for fast and accurate extraction of one-bond couplings from isotropic and partially aligned molecules, Magn. Reson. Chem. 53 (2015) 878–885, https://doi.org/10.1002/mrc.4276, https://onlinelibrary.wiley.com/doi/abs/10.1002/mrc.4276.

[29] D. Schulze-Sünninghausen, J. Becker, M.R.M. Koos, B. Luy, Improvements, extensions, and practical aspects of rapid ASAP-HSQC and ALSOFAST-HSQC pulse sequences for studying small molecules at natural abundance, J. Magn. Reson. 281 (2017) 151–161, https://doi.org/10.1016/j.jmr.2017.05.012, http://www.sciencedirect.com/science/article/pii/S1090780717301386.

[30] L. Mueller, Alternate HMQC experiments for recording HN and HC-correlation spectra in proteins at high throughput, J. Biomol. NMR 42 (2008) 129–137, https://doi.org/10.1007/s10858-008-9270-2, https://link.springer.com/article/10.1007/s10858-008-9270-2.

[31] M.P. Schätzlein, J. Becker, D. Schulze-Sünninghausen, A. Pineda-Lucena, J.R. Herance, B. Luy, Rapid two-dimensional ALSOFAST-HSQC experiment for metabolomics and fluxomics studies: application to a ^{13}C-enriched cancer cell model treated with gold nanoparticles, Anal. Bioanal. Chem. 410 (2018) 2793–2804, https://doi.org/10.1007/s00216-018-0961-6, https://link.springer.com/article/10.1007/s00216-018-0961-6.

[32] M.H. Levitt, R. Freeman, T. Frenkiel, Broadband heteronuclear decoupling, J. Magn. Reson. 47 (1982) (1969) 328–330, https://doi.org/10.1016/0022-2364(82)90124-X, https://www.sciencedirect.com/science/article/pii/002223648290124X.

[33] G.A. Morris, A. Gibbs, Heteronuclear polarization transfer by MLEV-16 isotropic mixing, J. Magn. Reson. 91 (1991) (1969) 444–449, https://doi.org/10.1016/0022-2364(91)90211-B, https://www.sciencedirect.com/science/article/pii/002223649190211B.

[34] A. Bax, D.G. Davis, MLEV-17-based two-dimensional homonuclear magnetization transfer spectroscopy, J. Magn. Reson. 65 (1985) (1969) 355–360, https://doi.org/10.1016/0022-2364(85)90018-6, https://www.sciencedirect.com/science/article/pii/0022236485900186.

[35] M. Kadkhodaie, O. Rivas, M. Tan, A. Mohebbi, A.J. Shaka, Broadband homonuclear cross polarization using flip-flop spectroscopy, J. Magn. Reson. 91 (1991) (1969) 437–443, https://doi.org/10.1016/0022-2364(91)90210-K, https://www.sciencedirect.com/science/article/pii/002223649190210K.

[36] F. Kramer, W. Peti, C. Griesinger, S.J. Glaser, Optimized homonuclear carr–purcell-type dipolar mixing sequences, J. Magn. Reson. 149 (2001) 58–66, https://doi.org/10.1006/jmre.2000.2271, https://www.sciencedirect.com/science/article/pii/S1090780700922717.

[37] J. Furrer, F. Kramer, J.P. Marino, S.J. Glaser, B. Luy, Homonuclear Hartmann-Hahn transfer with reduced relaxation losses by use of the MOCCA-XY16 multiple pulse sequence, J. Magn. Reson. 166 (2004) 39–46, https://doi.org/10.1016/j.jmr.2003.09.013, https://www.sciencedirect.com/science/article/pii/S1090780703003355.

[38] I.C. Felli, R. Pierattelli, S.J. Glaser, B. Luy, Relaxation-optimised Hartmann-Hahn transfer using a specifically Tailored MOCCA-XY16 mixing sequence for carbonyl–carbonyl correlation spectroscopy in ^{13}C direct detection NMR experiments, J. Biomol. NMR 43 (2009) 187–196, https://doi.org/10.1007/s10858-009-9302-6, https://link.springer.com/article/10.1007/s10858-009-9302-6.

[39] A.J. Shaka, C.J. Lee, A. Pines, Iterative schemes for bilinear operators; application to spin decoupling, J. Magn. Reson. 77 (1988) (1969) 274–293, https://doi.org/10.1016/0022-2364(88)90178-3, https://www.sciencedirect.com/science/article/pii/0022236488901783.

[40] S.J. Glaser, J.J. Quant, Homonuclear and heteronuclear hartmann—hahn transfer in isotropic liquids, in: W.S. Warren (Ed.), Advances in Magnetic and Optical Resonance, Academic Press, 1996, pp. 59–252, https://doi.org/10.1016/S1057-2732(96)80018-0.

[41] R.R. Ernst, G. Bodenhausen, A. Wokaun, Principles of Nuclear Magnetic Resonance in One and Two Dimensions, Clarendon Press, Oxford, 1987.

[42] T.E. Skinner, T.O. Reiss, B. Luy, N. Khaneja, S.J. Glaser, Application of optimal control theory to the design of broadband excitation pulses for high-resolution NMR, J. Magn. Reson. 163 (2003) 8–15, https://doi.org/10.1016/s1090-7807(03)00153-8, https://www.sciencedirect.com/science/article/pii/S1090780703001538.

[43] K. Kobzar, T.E. Skinner, N. Khaneja, S.J. Glaser, B. Luy, Exploring the limits of broadband excitation and inversion pulses, J. Magn. Reson. 170 (2004) 236–243, https://doi.org/10.1016/j.jmr.2004.06.017, https://www.sciencedirect.com/science/article/pii/S1090780704001995.

[44] T.E. Skinner, T.O. Reiss, B. Luy, N. Khaneja, S.J. Glaser, Reducing the duration of broadband excitation pulses using optimal control with limited RF amplitude, J. Magn. Reson. 167 (2004) 68–74, https://doi.org/10.1016/j.jmr.2003.12.001, https://www.sciencedirect.com/science/article/pii/S1090780703004221.

[45] T.E. Skinner, T.O. Reiss, B. Luy, N. Khaneja, S.J. Glaser, Tailoring the optimal control cost function to a desired output: application to minimizing phase errors in short broadband excitation pulses, J. Magn. Reson. 172 (2005) 17–23, https://doi.org/10.1016/j.jmr.2004.09.011, https://www.sciencedirect.com/science/article/pii/S1090780704003106.

[46] T.E. Skinner, K. Kobzar, B. Luy, M.R. Bendall, W. Bermel, N. Khaneja, S.J. Glaser, Optimal control design of constant amplitude phase-modulated pulses: application to calibration-free broadband excitation, J. Magn. Reson. 179 (2006) 241–249, https://doi.org/10.1016/j.jmr.2005.12.010, https://www.sciencedirect.com/science/article/pii/S1090780705004349.

[47] N.I. Gershenzon, K. Kobzar, B. Luy, S.J. Glaser, T.E. Skinner, Optimal control design of excitation pulses that accommodate relaxation, J. Magn. Reson. 188 (2007) 330–336, https://doi.org/10.1016/j.jmr.2007.08.007, https://www.sciencedirect.com/science/article/pii/S1090780707002352.

[48] K. Kobzar, T.E. Skinner, N. Khaneja, S.J. Glaser, B. Luy, Exploring the limits of broadband excitation and inversion: II, Rf-power optimized pulses, Journal of Magnetic Resonance 194 (2008) 58–66, https://doi.org/10.1016/j.jmr.2008.05.023.

[49] N.I. Gershenzon, T.E. Skinner, B. Brutscher, N. Khaneja, M. Nimbalkar, B. Luy, S.J. Glaser, Linear phase slope in pulse design: application to coherence transfer, J. Magn. Reson. 192 (2008) 235–243, https://doi.org/10.1016/j.jmr.2008.02.021, https://www.sciencedirect.com/science/article/pii/S1090780708000694.

[50] B. Luy, K. Kobzar, T.E. Skinner, N. Khaneja, S.J. Glaser, Construction of universal rotations from point-to-point transformations, J. Magn. Reson. 176 (2005) 179–186, https://doi.org/10.1016/j.jmr.2005.06.002, https://www.sciencedirect.com/science/article/pii/S1090780705001928.

[51] S. Ehni, B. Luy, A systematic approach for optimizing the robustness of pulse sequence elements with respect to couplings, offsets, and B_1-field inhomogeneities (COB), Magn. Reson. Chem. 50 (2012) S63–S72, https://doi.org/10.1002/mrc.3846, https://onlinelibrary.wiley.com/doi/abs/10.1002/mrc.3846.

[52] K. Kobzar, S. Ehni, T.E. Skinner, S.J. Glaser, B. Luy, Exploring the limits of broadband 90° and 180° universal rotation pulses, J. Magn. Reson. 225 (2012) 142–160, https://doi.org/10.1016/j.jmr.2012.09.013, https://www.sciencedirect.com/science/article/pii/S1090780712003126.

[53] T.E. Skinner, N.I. Gershenzon, M. Nimbalkar, W. Bermel, B. Luy, S.J. Glaser, New strategies for designing robust universal rotation pulses: Application to broadband refocusing at low power, J. Magn. Reson. 216 (2012) 78–87, https://doi.org/10.1016/j.jmr.2012.01.005, https://www.sciencedirect.com/science/article/pii/S1090780712000109.

[54] S. Ehni, B. Luy, BEBE^{tr} and BUBI: *J*-compensated concurrent shaped pulses for ^{1}H–^{13}C experiments, J. Magn. Reson. 232 (2013) 7–17, https://doi.org/10.1016/j.jmr.2013.04.007, https://www.sciencedirect.com/science/article/pii/S1090780713001006.

[55] S. Ehni, B. Luy, Robust INEPT and refocused INEPT transfer with compensation of a wide range of couplings, offsets, and B_1-field inhomogeneities (COB3), J. Magn. Reson. 247 (2014) 111–117, https://doi.org/10.1016/j.jmr.2014.07.010, https://www.sciencedirect.com/science/article/pii/S1090780714002109.

[56] D. Marion, K. Wüthrich, Application of phase sensitive two-dimensional correlated spectroscopy (COSY) for measurements of ^{1}H–^{1}H spin-spin coupling constants in proteins, Biochem. Biophys. Res. Commun. 113 (1983) 967–974, https://doi.org/10.1016/0006-291X(83)91093-8.

[57] A.J. Shaka, P.B. Barker, R. Freeman, Computer-optimized decoupling scheme for wideband applications and low-level operation, J. Magn. Reson. 64 (1985) (1969) 547–552, https://doi.org/10.1016/0022-2364(85)90122-2, https://www.sciencedirect.com/science/article/pii/0022236485901222.

[58] J. Yan, A.D. Kline, H. Mo, M.J. Shapiro, E.R. Zartler, A novel method for the determination of stereochemistry in six-membered chairlike rings using residual dipolar couplings, J. Org. Chem. 68 (2003) 1786–1795, https://doi.org/10.1021/jo020670i, https://pubs.acs.org/doi/abs/10.1021/jo020670i.

[59] A. Enthart, J.C. Freudenberger, J. Furrer, H. Kessler, B. Luy, The CLIP/CLAP-HSQC: pure absorptive spectra for the measurement of one-bond couplings, J. Magn. Reson. 192 (2008) 314–322, https://doi.org/10.1016/j.jmr.2008.03.009, https://www.sciencedirect.com/science/article/pii/S1090780708000967.

[60] W. Koźmiński, Simplified multiplet pattern HSQC-TOCSY experiment for accurate determination of long-range heteronuclear coupling constants, J. Magn. Reson. 137 (1999) 408–412, https://doi.org/10.1006/jmre.1998.1700, https://www.sciencedirect.com/science/article/pii/S1090780798917001.

[61] P. Nolis, T. Parella, Spin-edited 2D HSQC-TOCSY experiments for the measurement of homonuclear and heteronuclear coupling constants: Application to carbohydrates and peptides, J. Magn. Reson. 176 (2005) 15–26, https://doi.org/10.1016/j.jmr.2005.05.007, https://www.sciencedirect.com/science/article/pii/S109078070500162X.

[62] J.J. Titman, D. Neuhaus, J. Keeler, Measurement of long-range heteronuclear coupling constants, J. Magn. Reson. 85 (1989) (1969) 111–131, https://doi.org/10.1016/0022-2364(89)90324-7, https://www.sciencedirect.com/science/article/pii/0022236489903247.

[63] J.M. Richardson, J.J. Titman, J. Keeler, D. Neuhaus, Assessment of a method for the measurement of long-range heteronuclear coupling constants, J. Magn. Reson. 93 (1991) (1969) 533–553, https://doi.org/10.1016/0022-2364(91)90081-4, https://www.sciencedirect.com/science/article/pii/0022236491900814.

[64] M. Lin, M.J. Shapiro, Mixture analysis by NMR spectroscopy, Anal. Chem. 69 (1997) 4731–4733, https://doi.org/10.1021/ac970594x, https://pubs.acs.org/doi/full/10.1021/ac970594x.

[65] L. Verdier, P. Sakhaii, M. Zweckstetter, C. Griesinger, Measurement of long range H, C couplings in natural products in orienting media: a tool for structure elucidation of natural products, J. Magn. Reson. 163 (2003) 353–359, https://doi.org/10.1016/S1090-7807(03)00063-6, https://www.sciencedirect.com/science/article/pii/S1090780703000636.

[66] R.A.E. Edden, J. Keeler, Development of a method for the measurement of long-range ^{13}C–^{1}H coupling constants from HMBC spectra, J. Magn. Reson. 166 (2004) 53–68, https://doi.org/10.1016/j.jmr.2003.09.011, https://www.sciencedirect.com/science/article/pii/S109078070300332X.

[67] B. Görling, W. Bermel, S. Bräse, B. Luy, Homonuclear decoupling by projection reconstruction, Magn. Reson. Chem. 56 (2018) 1006–1020, https://doi.org/10.1002/mrc.4784, https://onlinelibrary.wiley.com/doi/abs/10.1002/mrc.4784.

[68] M.J. Thrippleton, J. Keeler, Elimination of zero-quantum interference in two-dimensional NMR spectra, Angew. Chem. Int. Ed. 42 (2003) 3938–3941, https://doi.org/10.1002/anie.200351947, https://onlinelibrary.wiley.com/doi/abs/10.1002/anie.200351947.

[69] D. Marion, M. Ikura, R. Tschudin, A. Bax, Rapid recording of 2D NMR spectra without phase cycling. Application to the study of hydrogen exchange in proteins, J. Magn. Reson. 85 (1989) (1969) 393–399, https://doi.org/10.1016/0022-2364(89)90152-2, URL: https://www.sciencedirect.com/science/article/pii/0022236489901522.

[70] Z. Starcuk, K. Bartusek, Heteronuclear broadband spin-flip decoupling with adiabatic pulses, J. Magn. Reson., Ser A 107 (1994) 24–31, https://doi.org/10.1006/jmra.1994.1043, https://www.sciencedirect.com/science/article/pii/S1064185884710436.

[71] M.R. Bendall, Broadband and narrowband spin decoupling using adiabatic spin flips, J. Magn. Reson., Ser A 112 (1995) 126–129, https://doi.org/10.1006/jmra.1995.1021, https://www.sciencedirect.com/science/article/pii/S1064185885710212.

[72] R. Fu, G. Bodenhausen, Broadband decoupling in NMR with frequency-modulated 'chirp' pulses, Chem. Phys. Lett. 245 (1995) 415–420, https://doi.org/10.1016/0009-2614(95)01037-A, https://www.sciencedirect.com/science/article/pii/000926149501037A.